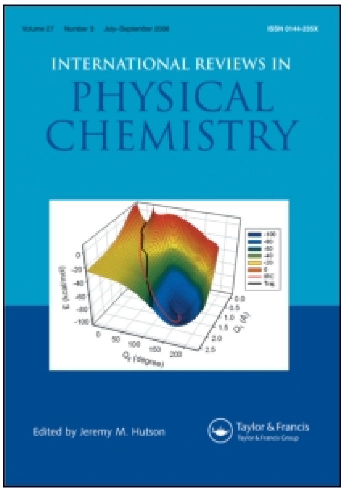

International Reviews in Physical Chemistry
Publication details, including instructions for authors and subscription information:
http://www.informaworld.com/smpp/title~content=t713724383

Spin-coupled valence bond theory

D. L. Cooper[a]; J. Gerratt[b]; M. Raimondi[c]
[a] Department of Inorganic, Physical and Industrial Chemistry, University of Liverpool, Liverpool, U.K.
[b] Department of Theoretical Chemistry, University of Bristol, Bristol, U.K. [c] Dipartimento di Chimica Fisica ed Elettrochimica, Universita di Milano, Milano, Italy

To cite this Article Cooper, D. L. , Gerratt, J. and Raimondi, M.(1988) 'Spin-coupled valence bond theory', International Reviews in Physical Chemistry, 7: 1, 59 — 80

To link to this Article: DOI: 10.1080/01442358809353205

URL: http://dx.doi.org/10.1080/01442358809353205

INTERNATIONAL REVIEWS IN PHYSICAL CHEMISTRY, 1988, VOL. 7, NO. 1, 59–80

Spin-coupled valence bond theory

by D. L. COOPER
Department of Inorganic, Physical and Industrial Chemistry,
University of Liverpool, P.O. Box 147, Liverpool L69 3BX, U.K.

J. GERRATT
Department of Theoretical Chemistry, University of Bristol,
Cantock's Close, Bristol BS8 1TS, U.K.

and M. RAIMONDI
Dipartimento di Chimica Fisica ed Elettrochimica,
Università di Milano, Via Golgi 19, 20133 Milano, Italy

In the spin-coupled description of molecular electronic structure, an N-electron system is described by N distinct—but non-orthogonal—orbitals, whose spins are coupled to the required resultant S in all possible ways. The coefficients of the basis functions comprising the orbitals and the coefficients of the different spin functions are fully optimized. The orbitals are frequently highly localized, and hence the model incorporates considerable electron correlation while retaining a high degree of visuality. The spin-coupled wave function is refined by non-orthogonal configuration interaction, and the final wave functions are of high quality but very compact. The various aspects of this theory are illustrated by a series of examples of increasing complexity: the H_2 molecule, the BeH molecule, the $^3B_1$ and $^1A_1$ states of CH_2 and the cycloaddition of CH_2 to ethenes, the π-electron system of benzene, and diazomethane (CH_2N_2). The results provide clear descriptions of the electronic structure and the associated processes. In benzene, the six π orbitals are highly localized, with far-reaching implications for the description of aromatic systems. The case of diazomethane shows that the central N atom takes part in *five* electron-pair bonds, and the same is true for a series of molecules such as N_2O, HCNO, NO_2, and CH_2NHO (nitrone), whose structures have long caused problems in valency theory.

1. Introduction

For thirty years or more, almost all our understanding of chemistry at a fundamental level has derived from the molecular orbital (MO) theory of electronic structure. That is, our view of molecular electronic structure has been based upon the Hartree–Fock or self-consistent field (SCF) model in which electrons move more-or-less independently of one another.

Such an approach undoubtedly has had a considerable number of successes to its credit, notably in the case of O_2 whose $^3\Sigma_g^-$ ground state is seen to fit naturally into a pattern established by the related closed-shell molecules N_2 and F_2. One of the widest uses of MO theory has been in the description of conjugated systems where, amongst other things, the important '$4n+2$' rule of aromaticity follows directly from the simplified version of the theory due to Hückel.

Nevertheless we have been uneasily aware of the shortcomings of this model, and as experimental techniques for the detailed elucidation of molecular processes have developed, these have become more constricting. There is, for example, no connection in MO theory between the molecular configurations and the asymptotic atomic or molecular fragment states, so that we do not have even a qualitative overview of the potential energy surfaces: the Hartree–Fock model breaks down for almost all bond dissociation processes since the configuration used to describe the molecule near the equilibrium geometry is usually inappropriate for the fragments.

These inadequacies can be remedied through the use of multiconfiguration wavefunctions. In general little is needed close to the equilibrium positions of the nuclei in the molecular ground state, except to provide added refinement to the MO wavefunction. However as the internuclear separations increase, the contribution of the SCF configuration rapidly diminishes, and usually becomes negligible. In addition there are a number of cases, particularly in transition-metal chemistry, where the Hartree–Fock model accounts for only a small fraction of the final wavefunction, even near the equilibrium geometry.

Equally, if not more, serious is the loss of any physical picture of the behaviour of correlated electrons. Once one goes beyond a single configuration, we no longer have any model of electronic structure to guide us. The best one can do is use the 'natural orbitals' from, say, a complete active space SCF (CASSCF) calculation, but these have fractional occupation numbers and so are difficult to interpret. Consequently almost every physical problem quickly devolves into technicalities of including ever larger numbers of configurations into giant configuration interaction (CI) wavefunctions.

If we allow ourselves to be guided by the physical processes under study, then we begin from wavefunctions of the constituent atoms (or other fragments) and from these construct wavefunctions for the required molecular states. This procedure introduces the correct physical features at the outset, and qualitatively at least provides us with a reasonably reliable view of the molecular potential energy surface as a whole.

The central characteristic of this approach is that wavefunctions of strongly interacting systems overlap one another. Since electrons are fermions, this non-orthogonality gives rise to exchange energies and these determine the form of the interactions between atoms and molecules.

The concepts introduced here can be used to provide a coherent explanation of a whole range of basic chemical phenomena. These include valency itself, the saturation of valency, directional bonding, multiple bonding and so on. The same ideas lead naturally to the concept of avoided intersections between two zeroth-order potential curves: if one curve is repulsive and the other attractive, we obtain an explanation—or sometimes a prediction—of potential energy barriers. If one curve is covalent and the other things, the important '$4n+2$' rule of aromaticity follows directly from the simplified version of the theory due to Hückel.

This 'classical valence bond (VB) theory' has thus provided us—at least on a qualitative level—with a whole set of concepts which find application throughout chemical physics. However numerical implementation of this theory has been disappointing: potential wells are too shallow and equilibrium bond lengths too long. The situation is improved by the addition of ionic structures, but the rate of convergence remains slow. Even more seriously, the number of ionic functions proliferates so rapidly—even in pre-eminently covalent situations such as hydrocarbon fragments—that the clarity and physical insight afforded by the original theory is lost.

Thus we have a seemingly well-founded theory which is successful at a qualitative or semi-empirical level, but whose *ab initio* results do not bear out these expectations. The key to this problem lies in the realization that one must allow for the essential *deformation* of the participating atoms or fragments as the molecules form. The bewildering presence of so many ionic structures is simply an attempt to remedy this deficiency.

The situation is fundamentally altered if the orbitals comprising the wavefunction are no longer of fixed atomic form, but instead are expanded as linear combinations of basis functions centred on all the nuclei of the system—much as in MO theory. Such orbitals are able to account for the distortions that occur as internuclear distances vary.

When we now construct an N-electron wavefunction from orbitals of this kind, there are a number of important further consequences. These are that the orbitals are necessarily non-orthogonal, and that each is occupied by a single electron only. In turn this makes it necessary to take into account the fact that there are several ways of coupling the spins of the individual electrons to give a required overall resultant S. Each mode of coupling the spins gives rise to a certain spin function $\Theta^N_{S,M;k}$ (which is specified in more detail below), and it is necessary to include a linear combination of all of them with variable coefficients in the total wavefunction.

An N-electron wavefunction constructed in this way from a configuration of N distinct non-orthogonal orbitals whose spins are coupled together in all allowable ways is termed a 'spin-coupled wavefunction'. It provides the basis for the modern form of valence bond theory. However it is worth stressing that the general approach typified by this wavefunction includes features hitherto associated with MO theory. Thus besides the use of an LCAO-type of expansion for the orbitals, the spin-coupled orbitals satisfy orbital equations and possess certain 'orbital energies'. The same orbital equations—of which there are now N—generate excited (or 'virtual') orbitals which are used to construct 'excited spin-coupled structures', which are in turn used in non-orthogonal configuration interaction calculations (to which we refer, not altogether accurately, as the 'VB stage') to refine the description afforded by the spin-coupled wavefunction and to provide the excited states. The resulting final wavefunctions are referred to as 'spin-coupled VB wavefunctions'.

In the spin-coupled wavefunction, both the form of the orbitals (that is, the coefficients in the linear combinations of the basis functions) and the coefficients of the spin functions are optimized simultaneously. The means by which this is achieved may be found in references [1–4]. It is worth stressing that the technical developments underlying this theory are new and are crucial. Hence some mention of them is necessary. These include extremely fast recurrence procedures for computing all the necessary 1-, 2-, 3- and 4-electron density matrices, and a powerful second-derivative method for minimizing the energy with respect to the coefficients for orbital and spin-coupling. We refer to this last as the 'stabilized Newton–Raphson method', and it is of interest to note that it was probably the first use of such a procedure in quantum chemistry.

The non-orthogonal CI part of the calculation (the 'VB stage') is accomplished by means of a very efficient program whose computational time varies as N^4. The bulk of the time needed for a complete spin-coupled VB calculation (aside from that spent in standard integral packages and transformations) is used at this stage. Careful comparisons show that these resources are competitive with those used by CASSCF-CI packages to obtain wavefunctions of comparable accuracy, particularly when several states of the same symmetry are required. In a number of cases it turns out that for an N-electron system, the spin-coupled wavefunction alone yields energies that are within one or two millihartrees of the CASSCF result for *all* configurations generated by distributing N electrons in N orthonormal orbitals.

In general, the programs outlined here are designed to make good use of the newer machines with large amounts of real or virtual memory, or fast input/output operations to external devices. Work is in hand to modify the procedures to exploit vector and parallel processing. The maximum number of correlated electrons that can be treated by the spin-coupled approach is about twelve on scalar machines, and will probably rise to 15–16 on vector and parallel processors.

The form of the N occupied spin-coupled orbitals is almost always that of deformed atomic functions, and consequently the orbitals are highly localized. The deformation consists of small amounts of delocalization onto neighbouring centres, and this is equivalent to the introduction of a little ionic character into the wavefunction. The excited orbitals possess corresponding features: they have the form of distorted atomic functions, becoming more diffuse as the energy increases. The contributions of the different spin functions highlight the behaviour of the wavefunctions in different regions of the potential surface. Generally speaking, at large internuclear separations, the mode of spin coupling is characteristic of reagents, but as the atoms or fragments approach, the orbitals deform and the coupling changes very rapidly to one characteristic of the newly formed molecule.

The plan of this review is to provide a survey of the results obtained with this theory. For this purpose we have selected a number of examples from recent work which display different aspects of the spin-coupled VB approach. In section 2 we present a minimum of formalism using H_2 and BeH as examples. Results for a variety of systems of increasing complexity are discussed in section 3. The power of the method in providing accurate results without losing visuality is demonstrated in the determination of the low-lying states of the CH_2 radical and its cycloaddition reaction with ethene. The versatility of the spin-coupled theory in providing a simple picture of the motion of correlated electrons is well demonstrated in the case of conjugated five- and six-membered ring systems, beginning of course with benzene. Finally the unexpected results for 1,3-dipolar molecules such as diazomethane (CH_2N_2) are discussed.

The number and variety of molecular systems that have been treated by the spin-coupled VB method is increasing rapidly. The nature of the physical insights that are revealed are frequently unexpected and differ both from that expected from MO theory and from classical VB theory. Nevertheless, the results have always made good physical and chemical sense, and accord well with known facts.

2. The spin-coupled VB wavefunction [1–4]

We consider an N-electron system, and write the spin-coupled wavefunction in the form

$$\begin{aligned}\Psi^0_{SM} &= \sum_{k=1}^{f^N_S} c_{Sk}\sqrt{N!}\mathscr{A}(\phi_1\phi_2\dots\phi_N\Theta^N_{S,M;k})\\ &\equiv\{\phi_1\phi_2\cdots\phi_N\} \qquad (1)\end{aligned}$$

In this equation the N spatial orbitals are denoted by $\phi_\mu(\mathbf{r})$, $\mu=1,2,\dots,N$, and the N-electron spin functions by

$$\Theta^N_{S,M;k}$$

The subscripts S and M indicate that this function is an eigenfunction of S^2 and S_z with eigenvalues $S(S+1)\hbar^2$ and $M\hbar$ respectively. The mode of coupling the individual electron spins is denoted by the index k, and the total number of allowed couplings is

$$f^N_S=\frac{(2S+1)N!}{(\frac{1}{2}N+S+1)!(\frac{1}{2}N-S)!} \qquad (2)$$

The totality of the different spin functions can be conveniently visualized by means of the 'branching diagram' which displays the construction of the $\Theta^N_{S,M;k}$ by means of successively coupling electron spins according to the rules for coupling angular momentum. In accordance with this procedure, the index k may be replaced by a more detailed designation as follows:

$$k \equiv (S_1 S_2 \ldots S_\mu \ldots S_{N-1}) \tag{3}$$

in which S_μ indicates the resultant spin after coupling the spin of electron μ. S_1 is of course always equal to $\frac{1}{2}$ and it is not necessary to specify S_N as this is just S itself.

The spin functions constructed in this way are normalized and orthogonal. This basis is known as the Yamanouchi–Kotani basis or—more simply—as the 'standard' basis of spin functions. However it should be stressed that this is not the only way of forming a basis of N-electron spin functions, and it is often convenient to use other bases [5].

The orbitals are expanded in a set of basis functions χ_p in the form

$$\phi_\mu = \sum_p c_{\mu p} \chi_p \tag{4}$$

The coefficients $c_{\mu p}$ and the spin coupling coefficients c_{Sk} are optimized simultaneously so as to minimize the total energy using the stabilized Newton–Raphson procedure.

As a simple illustration, consider the H_2 molecule. This system contains just two electrons. Correspondingly in spin-coupled theory there are two orbitals, and in the $X^1\Sigma_g^+$ ground state their spins are coupled to a net singlet spin, $S=0$. We denote the orbitals by σ_a and σ_b, and these are shown in figure 1 (*a*). It can be seen that they are essentially deformed H(1*s*) functions which are reflected into one another by the operation σ_h. The total wavefunction is in this case given by

$$\begin{aligned} \Psi(X^1\Sigma_g^+) &= \sqrt{(2!)}\mathscr{A}(\sigma_a\sigma_b\Theta^2_{0,0;1}) \\ &= \{\sigma_a(1)\,\sigma_b(2)+\sigma_b(1)\,\sigma_a(2)\}\sqrt{(1/2)}\{\alpha(1)\,\beta(2)-\beta(1)\,\alpha(2)\} \\ &= \{\sigma_a, \sigma_b\} \end{aligned} \tag{5}$$

This has the same form as the Heitler–London function, but the orbitals are now completely optimized. As the internuclear distance R increases, the deformation of the orbitals diminishes until eventually each becomes a pure H(1*s*) function. Thus in the limit of large R the spin-coupled theory correctly gives the Heitler–London function.

The potential curve given by the spin-coupled wavefunction is qualitatively correct over the whole range of internuclear distances, unlike its SCF counterpart, as shown in figure 1 (*b*). The degree of non-orthogonality between the orbitals σ_a and σ_b is shown by the overlap integral in figure 1 (*c*).

The picture of the covalent bond in this molecule is clear: to all intents and purposes, the bond is formed by the interaction between two deformed H(1*s*) functions. The deformation, though small, is crucial in providing 86% of the binding energy. The equilibrium internuclear distance R_e is within 0·015 Å of the experimental value. The fact that the orbitals are localized to a considerable degree enables the electrons to avoid one another, and consequently a significant amount of electron correlation is included in this model. The fact that the relevant orbitals are also non-orthogonal enables the electrons to interact with one another in such a way as to stabilize the molecule. The spin-coupled description thus incorporates the essential physics of bonding. Addition of extra structures does not alter this picture but merely adds an

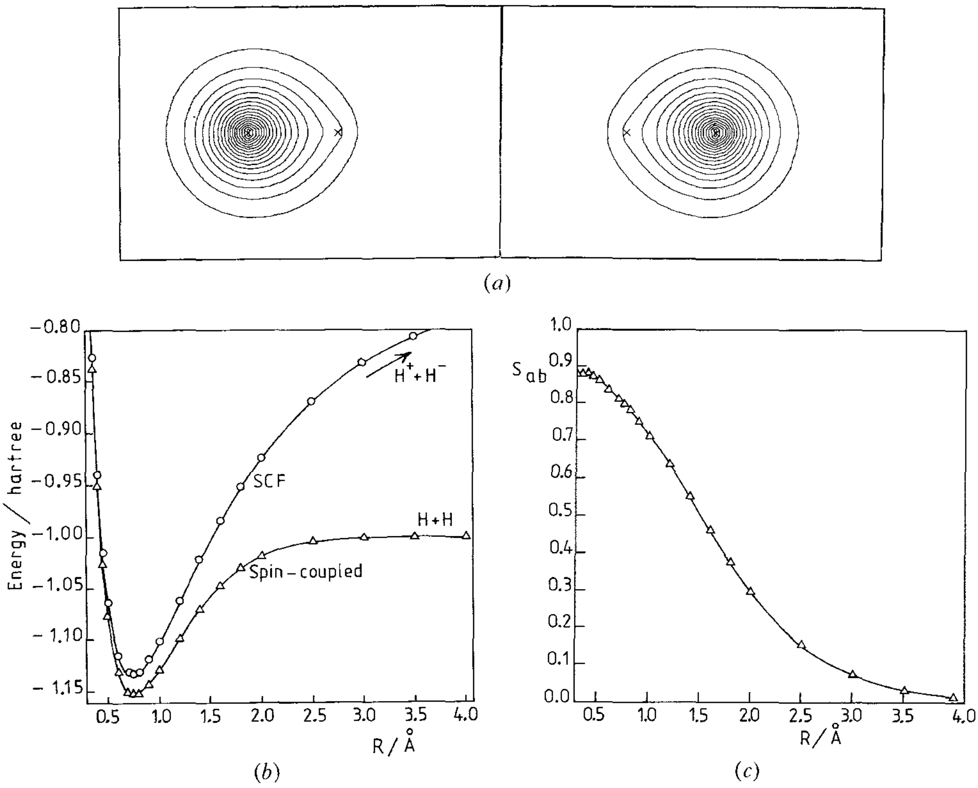

Figure 1. Orbitals and potential curves for $H_2(X\,^1\Sigma_g^+)$. (*a*) Spin-coupled orbitals σ_a and σ_b. The quantity plotted is $|\phi_\mu(\mathbf{r})|^2$ in a plane containing the two H atoms. (*b*) Spin-coupled and SCF potential curves. (*c*) The overlap integral between σ_a and σ_b. The orbitals are deformed H(1*s*) functions, the extent of the deformation decreasing with increasing internuclear distance *R*.

extra quantitative refinement—angular correlation in this case— and the final results can be made as accurate as desired.

The H_2 molecule does not exhibit some important features of the method, as there is only one spin function. The rôle of spin coupling is clearly illustrated by the $X\,^2\Sigma^+$ ground state of BeH. In this case the spin coupled wavefunction is of the form

$$\Psi=\sum_k c_{1/2k}\sqrt{(5!)}\mathscr{A}(\sigma_1\sigma_2\sigma_3\sigma_4\sigma_5\Theta^5_{1/2,M;k})$$
$$\equiv\{\sigma_1\sigma_2\sigma_3\sigma_4\sigma_5\} \qquad (6)$$

Since the net spin S is $\frac{1}{2}$, the total number of spin functions for this case is five (equation (2)). Orbitals σ_1 and σ_2 are almost entirely 1*s* and 1*s*′ orbitals of the Be atom. If these are coupled to a singlet spin throughout (which is reasonable), the number of possible spin functions decreases to two. At large R, orbitals σ_3 and σ_4 are completely localized on the Be atom and are also coupled to a singlet. Orbital σ_5 is an undeformed H(1*s*) function and accommodates the unpaired electron spin. As R decreases, a large change in the spin coupling occurs: orbital σ_3 distorts towards the H atom and recouples to form a singlet pair with σ_5, thus constituting the new Be–H bond. As a result at short Be–H separations, the unpaired electron is found in orbital σ_4. Somewhat unexpectedly, orbital σ_5 remains practically unchanged throughout [3,6]. These changes in the orbitals are shown in figure 2. Similar behaviour in the $\sigma(\mathrm{H}; 1s)$ orbital is observed in the case of LiH [7,8].

At long range, the spin-coupling coefficients $c_{\frac{1}{2}1}$, and $c_{\frac{1}{2}2}$ assume the values 0 and 1, characteristic of Be(^1S) and H($1s$). The change-over occurs surprisingly rapidly: for a wide range of values of R, the coupling remains that of the separated systems, but as R approaches a critical distance, ~4·5–3·5 a_0, the coefficients quickly assume values close to $\sqrt{3}/2$ and 1/2, which in the standard basis of spin functions corresponds to the pure 'molecular' coupling.

So far we have only discussed the form of the occupied orbitals. At convergence, each occupied orbital ϕ_μ is a solution of an equation of the type

$$F_\mu^{(\mathrm{eff})}\phi_\mu = \varepsilon_\mu \sigma_\mu \qquad (\mu = 1, 2, \ldots, N) \tag{7}$$

The $F_\mu^{(\mathrm{eff})}$ operators ($\mu = 1, 2, \ldots, N$) are all distinct and Hermitian. Each one gives rise to an orthonormal set of functions $\phi_\mu^{(i)}$ ($i = 0, 1, 2, \ldots$, etc.). One of these, $\phi_\mu^{(0)}$, is the occupied orbital already found, while the other solutions are excited or 'virtual' orbitals. However orbitals which belong to different stacks are not orthogonal. Thus

$$\begin{aligned} \langle \phi_\mu^{(i)} | \phi_\nu^{(j)} \rangle &= \delta_{ij} && \text{if } \mu = \nu \\ &= \Delta_{\mu\nu}^{(ij)} && \text{otherwise} \end{aligned} \tag{8}$$

It is important to note that the effective operators are constructed from quantities which consist of $N-1$ electrons only, so that each $\phi_\mu^{(i)}$ is determined in the field arising from all the *other* electrons. As a result, the orbitals are almost always highly localized.

Excited spin-coupled structures are formed by replacing one, two, three, or more occupied orbitals by virtual orbitals from their own stacks, i.e. $\phi_\mu \to \phi_\mu^{(i)}$, $\phi_\nu \to \phi_\nu^{(j)}, \ldots$ etc. The final spin-coupled wavefunctions are of the form

$$\Psi = C_0\{\phi_1\phi_2\ldots\phi_N\} + \sum_{i_1, i_2, \ldots} C(i_1 i_2 \ldots i_N)\{\phi_1^{(i_1)}\phi_2^{(i_2)}\ldots\phi_N^{(i_N)}\} \tag{9}$$

where $\{\phi_1\phi_2\ldots\phi_N\}$ represents the spin-coupled wave function (equation (1)), and $\{\phi_1^{(i_1)}\phi_2^{(i_2)}\ldots\phi_N^{(i_N)}\}$ stands for the excited structures. The energies and coefficients C_0, $C(i_1 i_2 \ldots i_N)$ are determined by constructing the Hamiltonian matrix over the spin-coupled structures $\{\phi_1^{(i_1)}\phi_2^{(i_2)}\ldots\}$ in (4) and diagonalizing. For this purpose we use an efficient N^4 VB program.

For the ground state, the spin-coupled structure (1) dominates the spin-coupled VB wavefunction for all geometries. The most important excited structures for introducing additional electron correlation are double excitations into very low-lying virtual orbitals. The final spin-coupled VB wavefunctions for excited states are also dominated by just one or two structures, and these are generally single excitations from the spin-coupled configuration.

Formally, equation (9) corresponds to an expansion of the exact wavefunction in N distinct orthonormal sets, each set being in some sense optimal for a particular electron coordinate. As a result we expect convergence of (9) to be much more rapid than if a single orthonormal set is employed—as in MO-CI wavefunctions. This is indeed found to be the case.

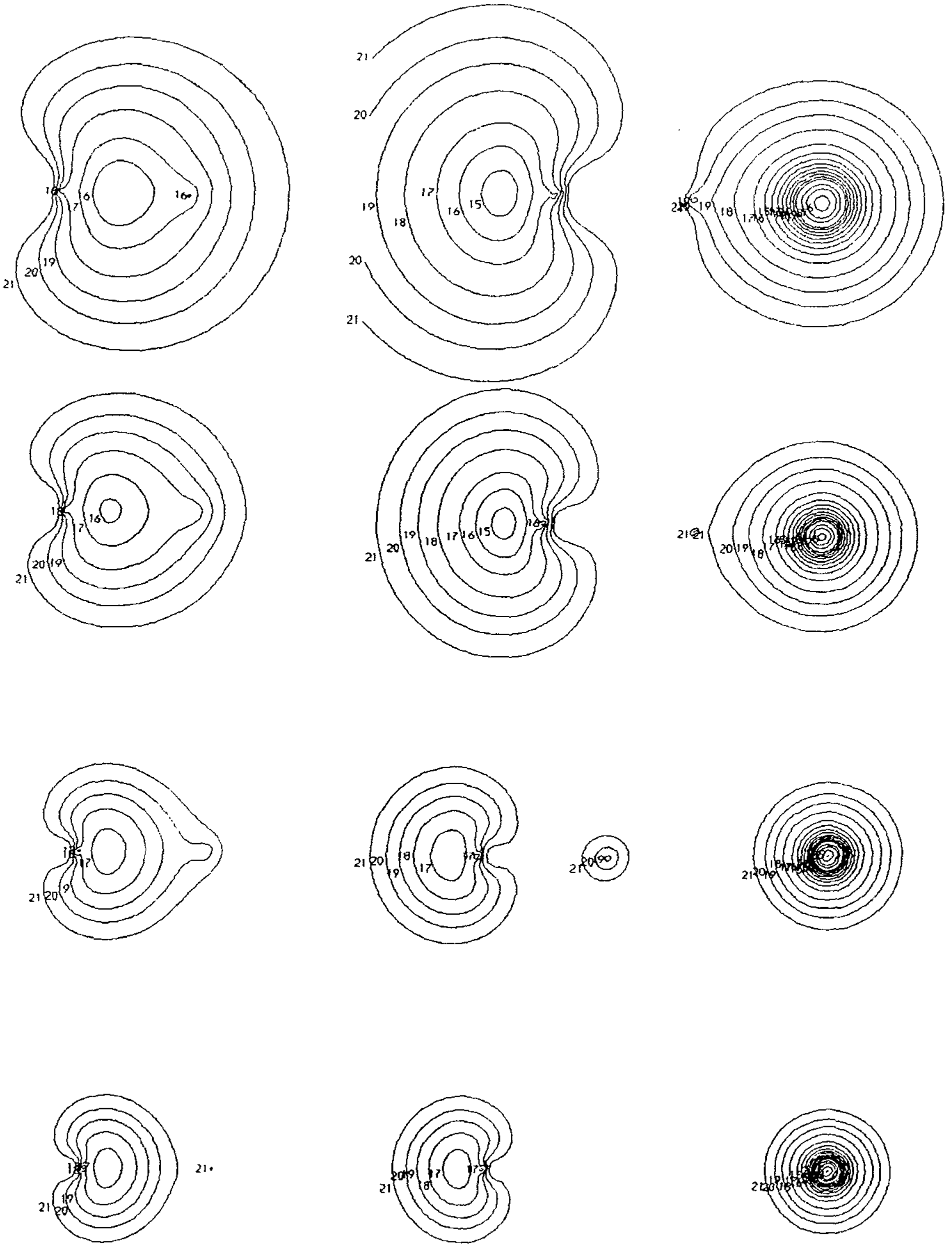

Figure 2. Electron density contours of valence orbitals in BeH for R values 2·5, 3·5, 5·0 and 6·0a_0. The three columns relate to $|\phi_\mu(\mathbf{r})|^2$ for $\mu = 3$, 4 and 5. The z axis points across the page from left to right with the H atom on the right.

For H_2, a small non-orthogonal CI calculation in which a single π orbital (x and y) is included from the a and b stacks provides 91% of the experimental D_e. A slightly larger calculation which includes the lowest-energy π orbital plus four σ orbitals from each stack yields 94% of the binding energy. This serves to show that almost all the correlation that can be provided by $\{\sigma, \sigma\}$ configurations is already included in the spin-coupled function. Greater accuracy can only be attained by inclusion of $\{\delta, \delta\}$ configurations, which provide higher-order angular correlation. However this hardly seems warranted, unless one were also to contemplate inclusion of non-adiabatic effects.

The spin-coupled VB calculations on low-lying $^2\Sigma^+$ states of BeH used a large 'universal even-tempered' basis set of Slater functions [9]. We have employed this as a standard basis set for a number of calculations on ground and excited states of diatomic molecules [10–13]. The VB calculation was carried out using the occupied orbitals, and from each stack corresponding to the valence electrons, the lowest three σ and π orbitals and the lowest δ orbital. All single and double excitations into these gives rise to 169 spatial configurations. In figure 3 we compare the dipole moment function calculated by the spin-coupled and spin-coupled VB methods with a *full*-CI calculation (on a smaller basis [14]). All three curves are similar out to an internuclear separation of $\sim 3a_0$. Beyond this, the spin-coupled wavefunction gives an absolute value which is too large. However the spin-coupled VB and full-CI results remain close; the remaining differences may reflect the larger basis set used here.

The sudden change in the spin coupling near $R = 4a_0$ is also reflected in the nature of the excited states. In classical VB theory the two lowest $^2\Sigma^+$ states of BeH are interpreted as arising from the interaction of two 'zeroth order' states: one stemming from Be(^1S)+H(1s), which is repulsive, and the other from Be(2s2p; ^3P)+H(1s) which provides the bonding. This results in an unusual low-lying $C^2\Sigma^+$ state which is stable and whose equilibrium bond length is almost twice that of the $X^2\Sigma^+$ state.

The existence of this state was also shown in earlier spin-coupled VB calculations [3], but because of unfavourable Franck–Condon factors, it was not observed directly for many years [15].

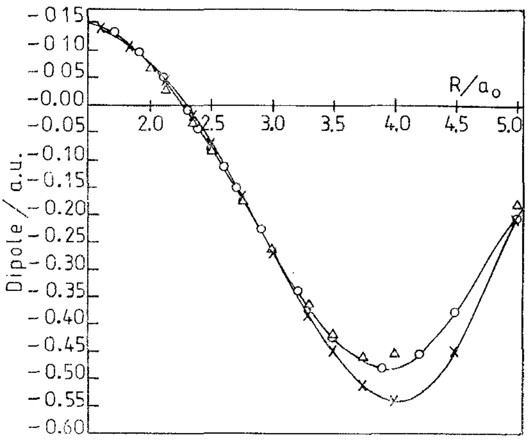

Figure 3. Dipole moment functions for BeH. (×) spin-coupled wavefunction. (Δ) spin-coupled VB wavefunction. (+) full CI calculation (smaller basis set). A negative value corresponds to Be^+H^-.

The case of BeH highlights the important rôle which the recoupling of the spins plays in providing a compact and visual description of molecular electronic structure and molecular processes. The suddent nature of the spin recoupling is an important phenomenon which we have observed in several reactive systems [16–19]: as reagents approach, there is a large range of intermolecular separations over which the system to all intents and purposes remains *un*changed. Then at a critical distance, a large recoupling takes place, and over a very short further distance ($1a_0$ or less), old bonds are broken and new ones—characteristic of the molecule or of the transition state—are formed.

3. Applications of spin-coupled VB theory

In this section, we give a survey of some of the results obtained using the approach described above.

3.1. *Low-lying states of the CH_2 radical and its addition to ethene* [19]

The determination of the equilibrium geometry of the $^3B_1$ ground state of CH_2 and of the separation between it and the lowest-lying singlet state ($^1A_1$) has received much attention from experimentalists and theoreticians. In this section we discuss two aspects of our spin-coupled VB calculations: we show first that spin-coupled VB theory gives a value for this singlet–triplet splitting which is in agreement with other theoretical studies and with the experimental value ($T_e = 9{\cdot}08 \pm 0{\cdot}18$ kcal mol^{-1} [20]). Secondly, we show that the chemical insight afforded by this model leads directly to a clear interpretation of the cycloaddition reaction of methylene with alkenes.

Spin-coupled calculations were carried out on the $^3B_1$, $^1A_1$ and $^1B_1$ states of CH_2 for a series of bond angles at intervals of 10°, keeping the C–H bond length fixed at $2{\cdot}1a_0$, and with two electrons (essentially the $1s^2$ core on C) accommodated in the first SCF orbital. The lowest energies (with no attempt at interpolation) were found at 130° ($^3B_1$), 100° ($^1A_1$), and 140° ($^1B_1$). The estimates of the equilibrium bond angles are in reasonable agreement with experiment [21].

Non-orthogonal CI calculations were carried out on the $^3B_1$ and $^1A_1$ states at the geometries used by Bauschlicher and Taylor in a full-CI calculation [22]. The spin-coupled VB calculations included a set of twelve orbitals, namely the occupied orbitals plus one virtual orbital from each stack. From them all, singly and doubly excited configurations were formed, as described in section 2. This gives rise to a list of 202 spatial configurations for both states. It is particularly important to include all the allowed modes of spin couplings, and upon doing so we obtain a set of 738 and 470 spin-coupled structures for the triplet and singlet states, respectively. The same list of configurations is used for both states, and the differences in the extent of the set of structures in the two cases is purely a result of the value of f_S^N (equation (2)).

The results are shown in table 1, together with a variety of other theoretical results using the same geometry and basis set. We obtain a value for the $^1A_1$–$^3B_1$ splitting of $12{\cdot}11$ kcal mol^{-1}, which is close to the full-CI result of $11{\cdot}97$ kcal mol^{-1}. This gives conviction to our final value of $9{\cdot}6$ kcal mol^{-1} which was obtained from the same set of structures but using a much more extended basis set.

We turn to the description of the states afforded by the spin-coupled wavefunction. Contour plots of the orbitals are shown in figure 4 for the $^3B_1$ and $^1A_1$ states. The orbitals for the $^1B_1$ state are similar to those of the $^3B_1$ state.

In the bent geometry of the $^3B_1$ state, the orbitals can be characterized as follows: orbital ϕ_1 is essentially a lobe of an sp^2 hybrid localized on the C atom and points

Table 1. Comparison of spin-coupled and spin-coupled valence bond results with the MO–CI calculations of Bauschlicher and Taylor [22]. All the calculations use the same geometry and basis set, but only five *d* components were included in the spin-coupled work (Taylor and Bauschlicher employed six).

Key for Wavefunctions

2C–SCF	Two-configuration SCF for $^1A_1$, one for $^3B_1$
SD–CI	Single and double excitations CI (single reference)
SD(Q)–CI	SD–CI plus corrections for quadruple excitations
2R–SD–CI	SD–CI with two reference configurations for $^1A_1$, one for $^3B_1$

	$^3B_1$–$^1A_1$ splitting (kcal mol^{-1})
Spin-coupled	13·27
Spin-coupled VB	12·11
SCF	26·14
2C–SCF	12·73
SD–CI	14·63
SD(Q)–CI	12·35
2R–SD–CI	12·20
CASSCF	12·82
Full CI	11·97

towards orbital ϕ_2 which is a deformed 1*s* orbital on one of the hydrogen atoms. Orbitals ϕ_3 and ϕ_4 are their counterparts localized about the second C–H bond. The overlap between ϕ_1 and ϕ_2, and between ϕ_3 and ϕ_4 is $\sim$0·8, and this highlights the strength of the two C–H bonds. Orbital ϕ_5 is centred on the carbon atom and is in essence the third lobe of the sp^2 hybrid. It points away from carbon. Orbital ϕ_6 is an almost pure C(2*p*) orbital and is perpendicular to the plane of the molecule. *None* of these orbital attributes is due to any preconceptions on our part—they arise naturally from minimization of the energy of the spin-coupled wavefunction.

In the $^1A_1$ state the orbitals are significantly different. Orbital ϕ_1 is in essence a lobe of an sp^3 hybrid pointing towards orbital ϕ_2 which is a deformed H(1*s*) function. Orbitals ϕ_3 and ϕ_4 are again the counterparts which describe the second C–H bond. However orbitals ϕ_5 and ϕ_6 are now the two remaining lobes of the sp^3 hybrid and describe the nonbonding electrons. This picture of the $^1A_1$ state differs markedly from that afforded by MO theory, according to which the two lone-pair electrons occupy a single lobe of what is essentially a C(sp^2) hybrid.

In MO theory a reliable description of the $^1A_1$ state cannot be obtained unless one begins from at least a two-configuration wavefunction of the type

$$\{\ldots(3a_1)^2\}-\mu^2\{\ldots(1b_1)^2\}$$

where $3a_1$ and $1b_1$ describe the lone-pair electrons. The need for two configurations of this kind becomes obvious when one considers the opening of the bond angle to 180°, for then $\mu\rightarrow 1$ and the x^2-y^2 component of a $^1\Delta_g$ state is correctly obtained. In the spin-

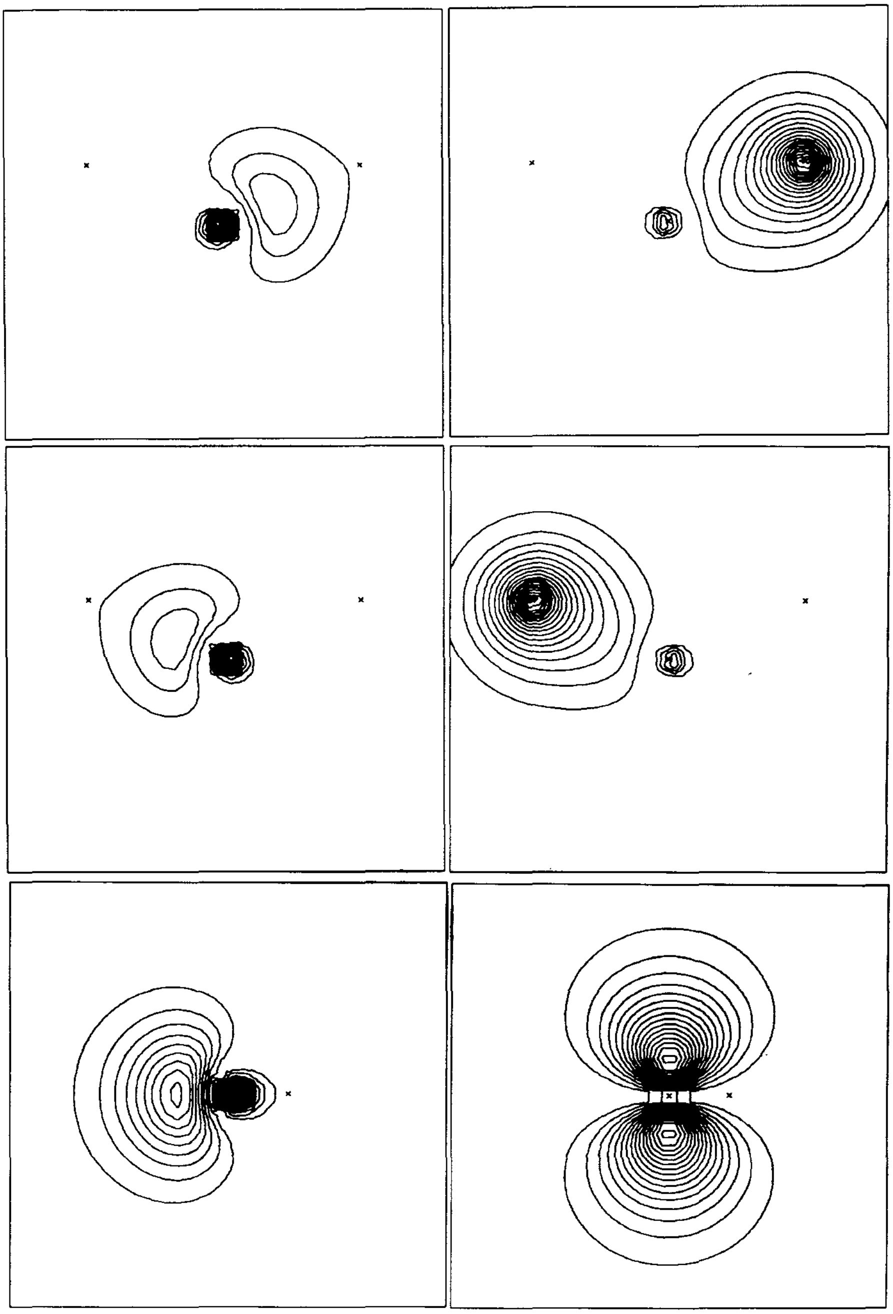

(a)

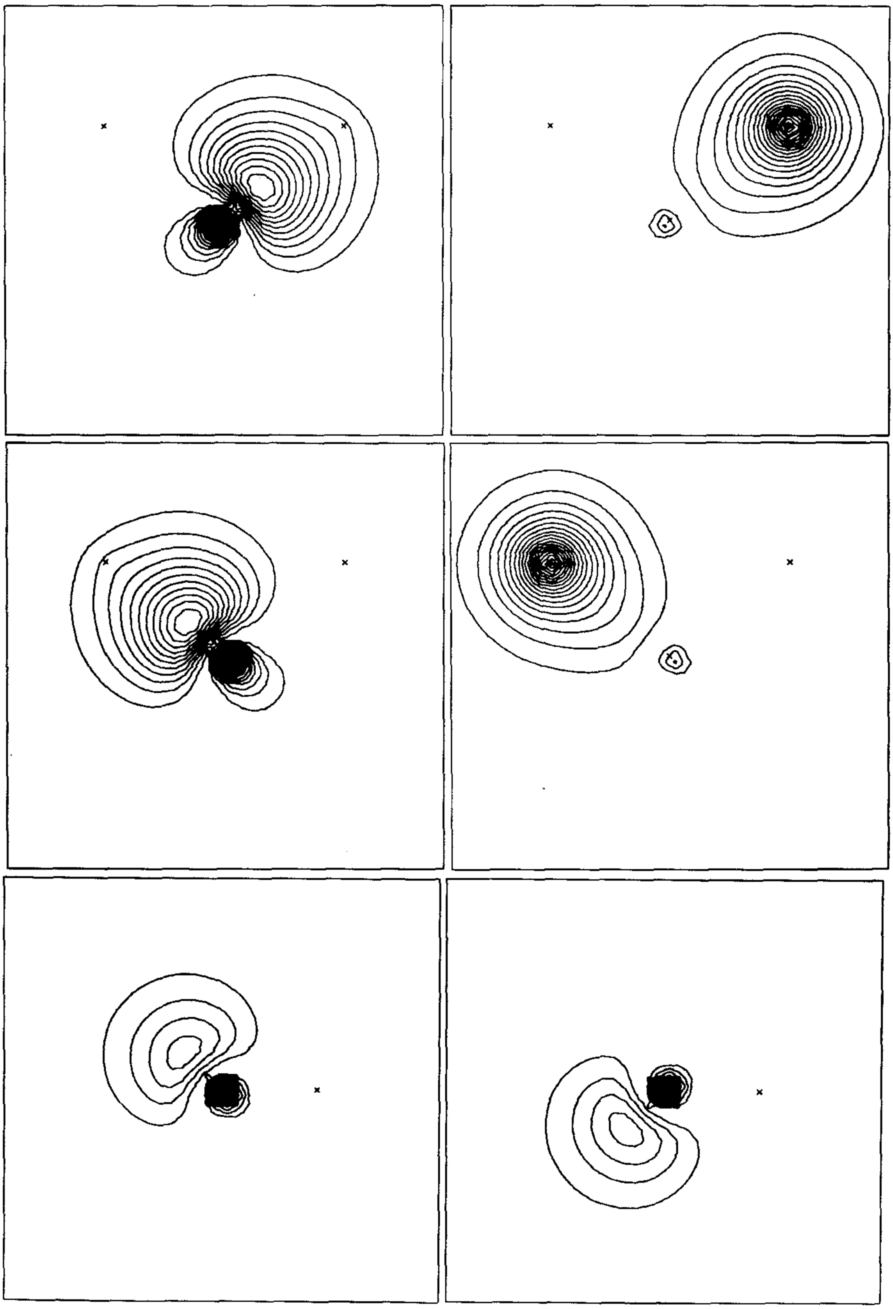

(b)

Figure 4. Contour plots of spin-coupled orbitals in CH_2: (a) the $^3B_1$ state, (b) the $^1A_1$ state. Orbitals ϕ_1–ϕ_4 are shown in the molecular (σ_v' mirror) plane and orbitals ϕ_5, ϕ_6 are shown in the σ_v mirror plane. We plot the square modulus of the orbitals $|\phi_\mu(\mathbf{r})|^2$.

coupled case we may decompose the orbitals ϕ_5 and ϕ_6 as follows:

$$\begin{aligned}\{\ldots\phi_5\phi_6\} &\simeq \{\ldots(a_1+\mu b_1)(a_1-\mu b_1)\}\\ &= \{\ldots(a_1)^2\} - \mu^2\{\ldots(b_1)^2\}\end{aligned}$$

which is of the same form as above, so the spin-coupled wavefunction automatically includes configurations which are necessary in the MO framework.

As the H–C–H angle increases in the $^1A_1$ state, the carbon orbitals involved in the C–H bonds become *sp* hybrids, while the orbitals occupied by the non-bonding electrons tend towards pure C(2*p*) orbitals, perpendicular both to the molecular axis and to each other. Closely related changes occur in the $^1B_1$ state. As a result of these variations, the $^1A_1$ and $^1B_1$ states become degenerate at 180° and form the two components of a $^1\Delta_g$ state.

In the light of these results, we consider the reactivity of CH_2 in terms of spin-coupled orbitals. Recall that while the present description of the $^3B_1$ state is similar to that of MO theory, the orbitals of the $^1A_1$ state possess different symmetries: instead of two non-bonding electrons in a single MO which lies in the plane of the molecule, there are now two distinct orbitals in a plane which is perpendicular to the molecule and bisects the H–C–H angle. This enables us to explain in a straightforward way the two kinds of reactions of methylene with substituted alkenes observed by Skell [23]:

$$CH_2(^1A_1) + RR'C{=}CR''R''' \rightarrow \text{one stereoisomer}$$

$$CH_2(^3B_1) + RR'C{=}CR''R''' \rightarrow \text{two stereoisomers}$$

When $CH_2(^1A_1)$ approaches the alkene, the two non-bonding electrons of the carbene are precisely in the right positions to overlap with the two orbitals which comprise the π system of the target. The electrons have the correct spin for permitting a sudden recoupling with the consequent formation of two new C–C bonds in a single step without allowing any rotation about C–C bonds. As a result, a single stereoisomer is formed. However, in the case of $CH_2(^3B_1)$, only the electron in the non-bonding lobe of the sp^2 hybrid can interact with the alkene. This orbital overlaps with one of the alkene π orbitals to form a single new C–C bond. The resulting diradical allows for much rotation about the C–C bonds, since the subsequent ring-closing step involves a triplet-to-singlet conversion and is slow. As a result two stereoisomers of the cyclopropane derivative are formed.

This description is different from that put forward by Hoffmann [24]. According to the Woodward–Hoffmann rules, the symmetric approach of $CH_2(^1A_1)$ to ethene along an axis of C_{2v} symmetry is forbidden: the interaction between the HOMO of the alkene and the LUMO of the carbene (the $1b_1$ orbital—which is essentially a C(2*p*) orbital perpendicular to the CH_2 plane) is antibonding. Nonetheless such reactions are common. The usual explanation for this anomaly [24, 25] is that the carbene approaches with its plane parallel to that of the alkene, and the attacking CH_2 group flips round when the new bonds are formed. Provided the attack is at one of the carbon atoms of the C=C bond (asymmetric path), the initial HOMO/LUMO interactions are bonding. However recall that in MO theory it is essential to use a two-configuration wavefunction for the $^1A_1$ state—consequently the application of symmetry rules to orbitals derived from a single-configuration SCF wavefunction is not convincing.

In MO theory only the spatial symmetry of the orbitals is assumed to be significant, and the electron spins play no rôle. In spin-coupled theory we attribute the stereospecificity of the additions to the part played by the electron spins.

In order to verify this model, we performed direct spin-coupled calculations for two paths on the lowest singlet potential energy surface. The first corresponds to the symmetric (C_{2v}) approach of CH_2 to ethene in which the plane of the methylene is perpendicular to that of ethene and bisects the C=C bond. The second is an asymmetric approach where the CH_2 impinges on one of the carbon atoms of ethene, the plane of the carbene being twisted to maximize the overlap of one of the singly occupied sp^3-like orbitals with one of the π orbitals of ethene.

In figure 5 we show the electronic energy of the two paths for both the SCF and spin-coupled descriptions. Particularly for the symmetric path, the difference between the SCF and spin-coupled results is very large. This shows that one only obtains agreement with the Woodward–Hoffmann rules at the SCF level. In the spin-coupled case, the reaction path has a barrier which turns out to be slightly lower for the asymmetric path.

The aim of these calculations is not to determine the height of the barrier, or to verify its existence, nor to define a minimum-energy path. We have performed crude calculations with the geometries of ethene and singlet methylene frozen at those of the isolated molecules. (To do better would require the incorporation of analytic energy derivatives [26] into the spin-coupled framework, which is a task of immediate priority.) Even so, the picture which emerges highlights features of spin-coupled theory and supports Skell's original interpretation of this reaction.

The mechanism of this reaction which emerges from these calculations for both the symmetric and asymmetric paths is as follows: in the asymptotic reactant region, the spin couplings and orbital overlaps show bonds localized on the separate molecular fragments. Once past the barrier, the spin couplings and overlaps change suddenly, and new C–C bonds characteristic of the cyclopropane ring form in a single step in accordance with the mechnanism of a cheletropic reaction [24]. It is interesting to observe that along both paths there is a point in the barrier region where the orbitals

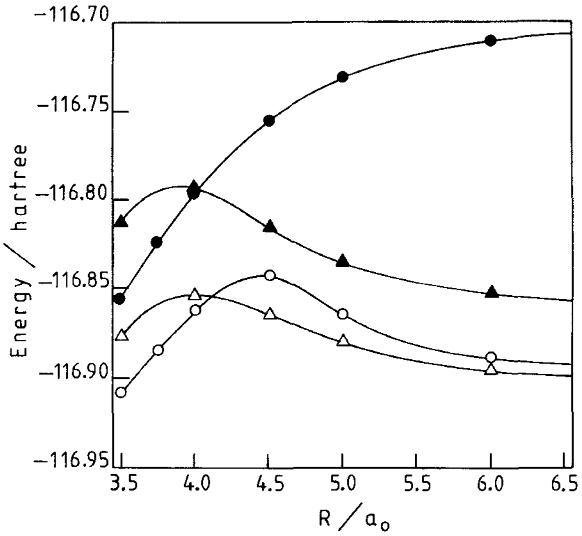

Figure 5. Energies relating to the symmetric (○, ●) and asymmetric (△, ▲) approach of methylene to ethene. The closed symbols refer to the SCF and the open symbols to the spin-coupled calculations.

originally centred on ethene deform and delocalize towards the more electrophilic CH_2. The orbitals centred on methylene are essentially unchanged. In addition, the CH_2 orbitals interact strongly with *two* partners: an ethene orbital and a methylene orbital. It is not hard to detect in this the operation of a hook or claw and consequently the word 'cheletropic' is appropriate for the picture which emerges from these calculations.

This study highlights the power of the spin-coupled VB approach in providing accurate numerical results and compact wavefunctions with a clear physical interpretation—in contrast to giant MO-CI wavefunctions which generally preclude the possibility of such insight.

3.2. *Aromatic systems: the benzene molecule* [27]

For a considerable number of years the generally accepted view has been that the aromatic character of benzene and other conjugated systems is best understood on the basis of a model in which the π electrons are delocalized. Although this description neglects any correlation between the electrons, it has been successful in explaining phenomena such as the '$4n+2$' rule of aromaticity, and in providing a general basis for the Woodward–Hoffmann rules of reactivity. However it has never been fully satisfactory: the concept of localized electron-pair bonds—and particularly their relocation in the course of reactions—remains remarkable useful in organic chemistry.

We have shown for the cycloaddition reactions of CH_2 with alkenes that the spin-coupled VB approach endorses this more 'chemical' view of the rôle of the electrons in molecular processes. Here we show further that the spin-coupled VB theory provides evidence which challenges the delocalized description of aromatic systems. Instead, the theory furnishes *ab initio* support for the view that the electrons in conjugated systems are well localized, and furthermore, that the special properties of such molecules arise from the particular mode of coupling the electron spins.

Spin-coupled calculations on the benene molecule were carried out with the 36 electrons of the σ framework accommodated in doubly-occupied molecular orbitals. The six π electrons are than described by six non-orthogonal orbitals, giving a total wavefunction of the form

$$\Psi = \sum_{k=1}^{5} c_{0k} \mathscr{A}\{\sigma_1^2\sigma_2^2\ldots\sigma_{18}^2\pi_1\pi_2\pi_3\pi_4\pi_5\pi_6\Theta^{36}_{0,0;f}\Theta^{6}_{0,0;k}\}$$

in which $\Theta^{36}_{0,0;f}$ is the spin function for the σ electrons, f here standing for f^{36}_0. The π orbitals were fully optimized together with the five spin coupling coefficients c_{0k}.

The converged wavefunction consists of six *highly localized* orbitals, the spins of which are coupled symmetrically around the carbon ring framework so as to give the overall ${}^1A_{1g}$ ground state. The orbitals possess identical energy and shape, and can be transformed into one another by successive rotations by $2\pi/6$. As shown in figure 6, the orbitals are essentially slightly deformed $C(2p_z)$ functions which are distorted symmetrically towards the neighbouring carbon atoms. This outcome emerges simply as a result of minimizing the total energy—no preconceptions as to the final form of the orbitals enter the calculation.

Because of the localized character of the orbitals, the electrons are able to avoid one another, so this model includes considerable electron correlation. This is reflected in the remarkably large energy lowering over the MO solution: 0·075 hartree (see table 2). However because the orbitals are non-orthogonal, the electrons are still able to influence one another directly. In particular when there is a magnetic field

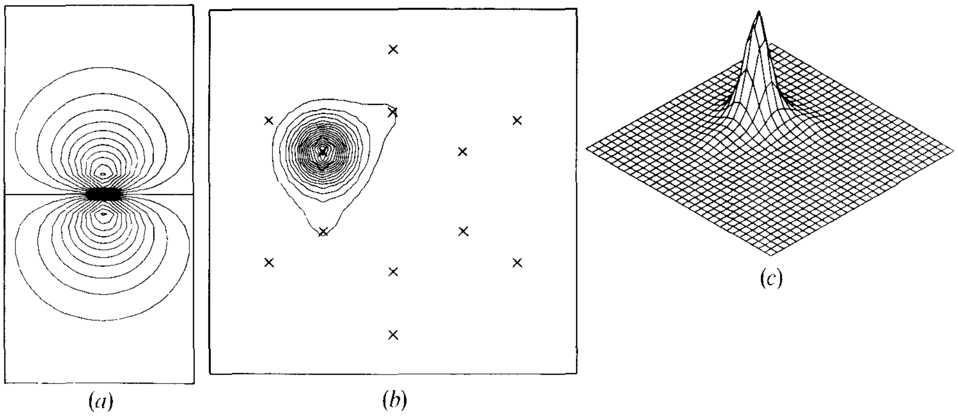

Figure 6. One of the spin-coupled orbitals ϕ_μ in benzene. The others are generated from it by successive rotations by $2\pi/6$. (a) Contours of $\phi_\mu(\mathbf{r})$ in a σ_v mirror (i.e. in a plane perpendicular to the molecular frame and containing two C–H bonds). (b) Contours of $|\phi_\mu(\mathbf{r})|^2$ in a plane $1a_0$ above the C_6H_6 plane. The nuclei below are denoted by ×. (c) An isometric view corresponding to (b).

perpendicular to the plane of the molecule, the non-orthogonality ensures the existence of a 'hopping probability', so that the six electrons may move around the ring in a concerted fashion.

The spin-coupled model provides a simple picture of the motion of *correlated* electrons in such systems. In addition, it is also able to account for the anisotropy in the diamagnetic susceptibility of benzene (the so-called 'ring currents')—a feature hitherto associated with delocalized electrons.

Conformation of the validity of the spin-coupled description is provided by carrying out a 'full VB' calculation which includes all possible structures of ${}^1A_{1g}$ symmetry formed from the six occupied π orbitals. This consists of all singly-, doubly- and triply-ionic structures and gives rise to a total of 175 functions. As seen from table 2, the further energy lowering which results from the inclusion of these structures is negligible. One of the most unacceptable aspects of the classical valence bond description has been the apparent predominance of such highly unphysical contributions. In spin-coupled theory we see that they are unnecessary. The deformation of the orbitals from pure atomic form, though small, is crucial.

The spin coupling coefficients c_{0k} were determined using the standard basis of spin functions. Upon transforming to the Rumer basis, which is widely used in classical VB theory, we find that the weights of the two Kekulé and three para-bond ('Dewar') structures in table 3 are close to the values given many years ago by Pauling in his original—and much simplified—calculation [28].

Table 2. Total energies for benzene using [3s2p/2s] and [3s3p/2s] contracted Gaussian basis sets.

SCF	−229·995 39	−230·001 50
Spin-coupled	−230·070 43	−230·076 27
Spin-coupled VB†	−230·077 39	−230·083 24

† 175 structures. See the text.

Table 3. Occupation numbers of the spin functions in the Rumer Basis. Functions 1 and 4 correspond to the Kekulé structures, whereas 2, 3 and 5 correspond to para-bond (Dewar) structures.

Rumer function	Occupation number
1	0·4028
2	0·0648
3	0·0648
4	0·4028
5	0·0648

These findings have been confirmed, and their significance broadened, by additional calculations on a series of five- and six-membered heterocyclic rings [29, 30]. For the six-membered pyridine, pyrazine, pyrimidine and pyridazine, the orbitals are highly localized much as in benzene. The energy lowerings over the MO solutions are now very large: 212 kJ mol^{-1} in the case of pyridine, for example. The contributions of the different spin couplings in these molecules generally conform to the pattern found for benzene, with the proviso of a marked preference for $C=N$ bonds—and this seems entirely reasonable.

For all these systems we can define a 'resonance energy' which is the difference between the full spin-coupled solution based on all the spin couplings and the energy of the single most important structure. Thus pyridine has a resonance energy of 92 kJ mol^{-1}, furan 11 kJ mol^{-1}, and pyrrole 31 kJ mol^{-1}.

3.3. *The electronic structure of diazomethane* (CH_2N_2) [31]

Diazomethane is one of a large class of molecules, along with N_2O, HCNO, NO_2 and ozone, whose structure has caused problems for valency theory. The accepted fashion of representing this molecule is:

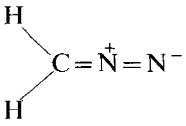

with a smaller contribution from a similar structure with a negative charge on the carbon atom. However this would appear to predict a large dipole moment, whereas the value is 1·45 D [32]. MO-CI [33] and perfect pairing GVB calculations [34] conclude that diazomethane is largely a diradical of the type

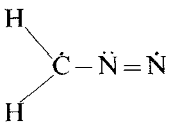

which flies in the face of the chemical evidence.

Spin-coupled calculations were carried out taking into account just four electrons which are described by four out-of-plane ('π') orbitals. The other electrons are accommodated in doubly occupied in-plane orbitals of the molecular ('σ') framework. However a more sophisticated description would need to take into consideration the in-plane $2p$ functions on the two nitrogen atoms.

The calculated energies and dipole moments for this molecule are listed in table 4. The spin-coupled wavefunction yields an energy 0·045 hartree lower than that of the SCF description: further lowering of the energy on including all structures with double occupancy ('ionic' structures) is negligible.

Table 4. Total energies and dipole moments for diazomethane.

	Energy (a.u.)	Dipole moment (debye)
SCF	−147·6572	0·99
Spin-coupled	−147·7024	1·12
Spin-coupled VB†	−147·7026	1·12

† Includes spin-coupled and all ionic structures.

The four orbitals are shown in figure 7. They have the form of deformed $2p$ functions: orbital ϕ_1 is localized on the C atom but is distorted towards the central N atom, N_a; orbital ϕ_2 is localized on N_a but is distorted towards C; ϕ_3 is also localized in N_a but is distorted towards the terminal nitrogen atom, N_b; and lastly orbital ϕ_4 is localized on N_b but is deformed towards N_a. The spin coupling coefficients in the standard basis are 0·300 and 0·954, with the larger number corresponding to the perfect pairing function $\{(\phi_1, \phi_2)(\phi_3, \phi_4)\}$. Thus the overwhelming character of the molecule is one where there are two conventional bonds, one between C and N_a giving a net C–N double bond, and a second between N_a and N_b, giving essentially a net N–N *triple* bond as follows:

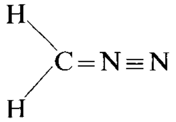

This is reflected in the observed N–N bond length of 1·14 Å which is remarkably close to that of isolated N_2 (1·10 Å). The second spin function, which gives rise to some diradical character, contributes less than 10% to the whole.

The unexpected nature of this result arises from the fact that the two orbitals which stem from the central N atom, ϕ_2 and ϕ_3, have an overlap of no less than 0·925—and yet they are *not* coupled with each other to give a singlet as one would expect. The essentially normal character of the bonding in diazomethane arises from the fact that a $2p_\pi$ orbital originating from the central nitrogen atom is allowed to 'split'—i.e. the bonding arises entirely from the allowance for *electron correlation*, both in the isolated atom and in the molecule. If the two electrons were accommodated in a single orbital, either in the classical VB or MO framework, the problem would remain.

From this one can see that a similar description is likely to apply to NO_2. If the $2p_\pi$ orbital which originates from the N atom is allowed to split in the same way, it is

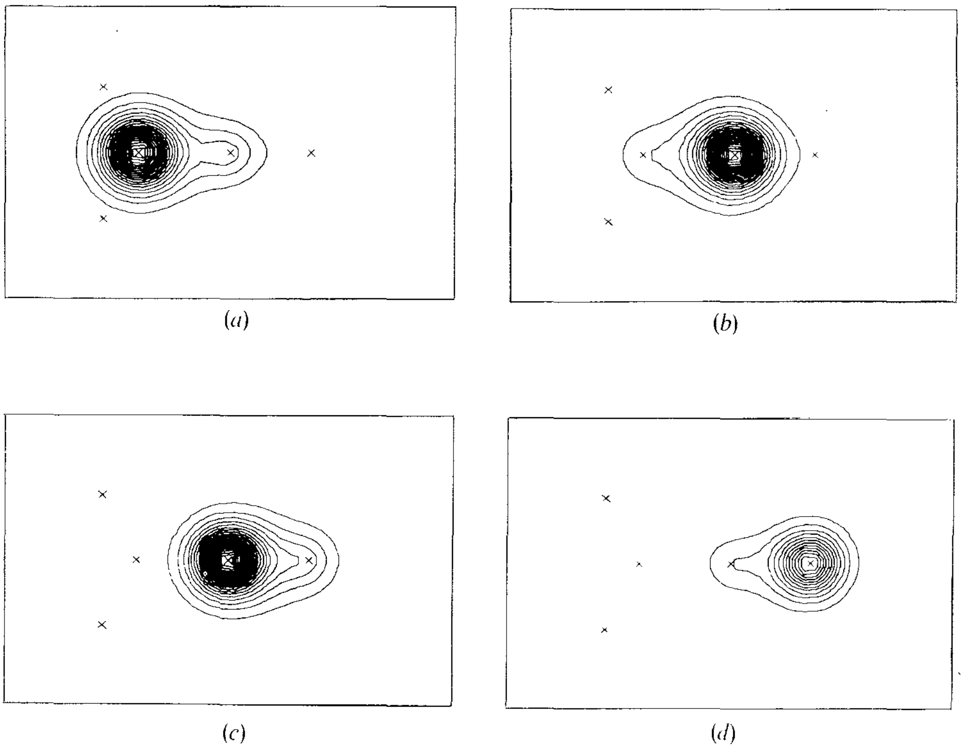
(a) (b) (c) (d)

Figure 7. Spin-coupled orbitals for the four π electrons (B_1 symmetry) of diazomethane. The quantity plotted is the square modulus $|\phi_\mu(\mathbf{r})|^2$ in a plane $1a_0$ above the molecular plane. The positions of the nuclei in the plane below are denoted by crosses. (a) ϕ_1, (b) ϕ_2, (c) ϕ_3, (d) ϕ_4.

possible to form two reasonable N–O double bonds. The awkward resonance structures of classical VB theory are then unnecessary, and the embarrassing symmetry instability of MO theory—which occurs when one bond is lengthened and then restored—does not arise. Similar considerations may apply to N_2O, O_3 and SO_2 which have long been the source of unresolved valency problems.

The GVB calculations were carried out using a larger number of active orbitals than here. However the 'generalized valence bond' wavefunction is based upon the 'strong orthogonality' constraint, and at least in this case, is untenable: the *smallest* overlap (that between orbitals localized on C and N_b) is 0·433. It is therefore difficult to take seriously any calculation which imposes such constraints, and consequently all of the GVB calculations on other 1,3-dipoles should be treated with suspicion.

This work points to the following general conclusion: in the formation of multiple bonds with neighbouring atoms, we may if necessary quite properly assign a formal valency of *five* to the nitrogen atom. This is possible because $2p$ orbitals only are involved, and the effect is essentially due to electron correlation. This does not affect the arguments concerning the instability of molecules such as NCl_5, since here the stereochemistry dictates that $3d$ orbitals would have to play a central rôle, but these are too high in energy.

4. Conclusions

In the review we have attempted to survey some of our recent results. The examples we have chosen demonstrate the kinds of new insights afforded by the spin-coupled VB theory, and the accuracy obtainable. One aspect which we have not covered is that of excited states of molecules: in several cases we have obtained 10–20 states of the same symmetry, spanning an energy range of up to 40 eV. In the case of the doubly-charged cation of H_2O [35], for example, we obtained entire potential surfaces for several states, each correctly describing all the dissociation processes.

After a long period of relative obscurity, valence bond theory—in the form presented here—is making an impact upon the way we think about molecular electronic structure and processes.

References

[1] Gerratt, J., 1971, *Adv. Atom. Molec. Phys.*, **7**, 141.
[2] Pyper, N. C., and Gerratt, J., 1977, *Proc. Roy. Soc.* A, **355**, 407.
[3] Gerratt, J., and Raimondi, M., 1980, *Proc. Roy. Soc.* A, **371**, 525.
[4] Cooper, D. L., Gerratt, J., and Raimondi, M., 1987, *Adv. Chem. Phys.*, **69**, 319.
[5] Pauncz, R., 1979, *Spin Eigenfunctions* (New York and London: Plenum).
[6] Allan, N. L., and Cooper, D. L., 1987, *J. Chem. Soc. Faraday Trans.*, *2*, **83**, (9), 1675.
[7] Cooper, D. L., Gerratt, J., and Raimondi, M., 1985, *Chem. Phys. Lett.*, **118**, 580.
[8] Cooper, D. L., and Allan, N. L., 1987, *J. Chem. Faraday Trans.*, *2*, **83**, 449.
[9] Cooper, D. L., and Wilson, S., 1983, *J. chem. Phys.*, **78**, 2456.
[10] Cooper, D. L., Gerratt, J., and Raimondi, M., 1985, *Molec. Phys.*, **56**, 611.
[11] Cooper, D. L., Gerratt, J., Ford, M. J., and Raimondi, M., 1986, *Phys. Rev.* A, **34**, 1752.
[12] Barnard, S. A., Ford, M. J., Cooper, D. L., Gerratt, J., and Raimondi, M., 1987, *Molec. Phys.*, **60**, 1193.
[13] Penotti, F., Cooper, D. L., Gerratt, J., and Raimondi, M., 1987, *Calculation of Potential Energy Curves of Excited* $^2\Pi$ *States of the CH Radical* (to be published).
[14] Larsson, M., 1985, *Physica Scripta*, **32**, 97.
[15] Colin, R., Dreze, C., and Steinhauer, M., 1983, *Can. J. Phys.*, **61**, 641.
[16] Raimondi, M., and Gerratt, J., 1983, *J. chem. Phys.*, **79**, 4339.
[17] Cooper, D. L., Gerratt, J., and Raimondi, M., 1986, *Chem. Phys. Lett.*, **127**, 600.
[18] Walters, S. G., Penotti, F., Gerratt, J., and Raimondi, M., 1987, *Molec. Phys.*, **61**, 1341.
[19] Sironi, M., Cooper, D. L., Gerratt, J., and Raimondi, M., 1987, *J. Chem. Soc. Faraday Trans.*, *2*, **83**, (9), 1651.
[20] McKellar, A. R. W., Bunker, P. R., Sears, T. J., Evenson, K. M., Saykally, R. J., and Langhoff, S. R., 1983, *J. chem. Phys.*, **79**, 5251.
[21] Herzberg, G., and Johns, J. W. C., 1966, *Proc. Roy. Soc.* A, **295**, 107; Bunker, P. R., and Jensen, P., 1983, *J. chem. Phys.*, **79**, 1224.
[22] Bauschlicher, C. W., and Taylor, P. R., 1986, *J. chem Phys.*, **85**, 6510.
[23] Skell, P. S., and Woodworth, 1956, *J. Am. Chem. Soc.*, **78**, 4496; Skell, P. S., and Garner, A. Y., 1956, *Ibid.*, **78**, 5430; Etter, R. M., Skovronek, H. S., and Skell, P. S., 1959, *J. Am. Chem. Soc.*, **81**, 1008.
[24] Hoffmann, R., 1968, *J. Am. Chem. Soc.*, **90**, 1475; see also Closs, G. L., 1968, *Topics Stereochem.*, **3**, 193.
[25] Fleming, I., *Frontier Orbitals and Organic Chemical Reactions* (London: John Wiley), p. 95.
[26] Gerratt, J., and Mills, I. M., 1968, *J. chem. Phys.*, **49**, 1730.
[27] Cooper, D. L., Gerratt, J., and Raimondi, M., 1986, *Nature, Lond.*, **323**, 699.
[28] Pauling, L., 1933, *J. chem. Phys.*, **1**, 280.
[29] Cooper, D. L., Gerratt, J., Raimondi, M., and Wright, S. C., 1987, *J. Am. Chem. Soc.* (in the press).
[30] Cooper, D. L., Gerratt, J., Raimondi, M., and Wright, S. C., 1987, *J. Am. Chem. Soc.* (in the press).

[31] Cooper, D. L., Gerratt, J., Raimondi, M., and Wright, S. C., 1987, *Chem. Phys. Lett.*, **138,** 296.

[32] Cox, A. P., Thomas, L. F., and Sheridan, J., 1958, *Nature, Lond.*, **181,** 1000.

[33] Hiberty, P. C., and Leforestier, C., 1978, *J. Am. Chem. Soc.*, **100,** 2012.

[34] Walch, S. P., and Goddard, W. A., 1975, *J. Am. Chem. Soc.*, **97,** 5319.

[35] Cooper, D. L., Gerratt, J., Raimondi, M., and Sironi, M., *J. chem. Phys.*, **87,** 1666.